Research on Chemical Intermediates (2020) 46:2457–2479
https://doi.org/10.1007/s11164-020-04101-2

IR and Raman spectra with Gaussian-09 molecular analysis of some other parameters and vibrational spectra of 5-fluoro-uracil

J. S. Singh[1]

Received: 14 November 2019 / Accepted: 7 February 2020 / Published online: 2 March 2020

Abstract
Recorded IR and Raman spectra of 5-fluoro-uracil have been analyzed with the carried out theoretical computation by Gaussian-09 [DFT/B3LYP/6-311++G**] and GAR2PED software. In the assignment of fundamental modes, the GAR2PED software has been used to calculate the PEDs. HOMO–LUMO energy gap study supports the possibility of charge transfer in biomolecule. Electrostatic potential plotting with iso-surface plot and the mappings of electron density with molecular electrostatic potential have been made for the concept of charge distribution in molecules as the sites of nucleophilic reactions and electrophilic effect. The DFT calculations have been employed to yield the atomic polarizability tensor charges, Mulliken atomic charges, molecular structure and thermodynamic functional properties of the biomolecule. The assignment has been made in the two species for the normal mode of the fluoro group substituent on pyrimidine ring.

Keywords IR Raman spectra · DFT · HOMO–LUMO · MEPs/ESPs · Thermodynamics

Introduction

5-Fluoro-uracil is an aromatic organic compound having heterocyclic shape. Uracil is a naturally occurring pyrimidine derivative, which is an essential constituent of ribonucleic acid (RNA). In deoxyribonucleic acid (DNA), uracil is replaced by 5-methyl-uracil (thymine). The halogenated uracils act as the anticancer agents. The derivatives of uracil or 5-substituted uracils significantly change their chemical/physical behavior and optical properties in vivo and bioactivity. It has been found to exhibit significant role in pharmacological activities. Therefore, the pyrimidine

✉ J. S. Singh
jssaec@rediffmail.com; jssaec@gmail.com

[1] Department of Physics, Jamia Millia Islamia (Central University), New Delhi 110025, India

derivatives are extensively used by the medical community as follows: 5-fluoro-uracil is normally used as an anticancer drug; 5-trifluoro-methyl-uracil and 5-iodo-uracil show anti-viral activity so that the study of uracil and their derivatives is very interesting due to the spectroscopic properties and bioactivities [1–3], and these are commonly used as drugs for anti-HIV viruses and anti-carcinogenic [4–8]. Anti-carcinogenic drug, 5-fluoro-uracil as fluorinated pyrimidine antimetabolite, is normally used in the treatment of solid tumors and colorectal carcinoma [4, 5]. Moreover, all these derivatives as 5-substituted uracils are tested as anti-HIV and anti-tumor drugs [6, 8]. Here, the study based on fluoro-uracil has been made.

This work is to carry out the DFT computations of 5-fluoro-uracil for the structural geometries, molecular charges and the vibrational frequencies using DFT [B3LYP] method on the 6-311++G** basis set available in Gaussian-09 programs [24]. All normal vibrational modes have been assigned using the computed vibrational modes and related parameters are obtained from the Gauss View-5.09 [25] of Gaussian-09 program package [24] and the PEDs are obtained with help of GAR2PED software [26]. Here, the reactivity of 5-fluoro-uracil for the charge transfer, intramolecular hydrogen bonding, analysis of orbital energies and other analysis is also investigated.

This article is the related study of fluoro group substitution on pyrimidine ring of uracil. The vibrational studies for 5-substituted uracils [9–24] have been made by several authors that are still required more value-added study on the fifth position of pyrimidine ring, which is not fully decided and is required a further study.

Materials and methods

(A) *Experiment:* A very small quantity (~1 mg) of 5-fluoro-uracil powder of spectral grade was obtained from the Aldrich chemical Company (USA) and used as such for recording the IR and Raman spectra. Its spectra were recorded for spectroscopic analysis in solid phase on room temp (23 °C). The experimental spectrum given Fig. 1a was recorded on room temp (23 °C) within the region 400–4000 cm^{-1} by the Fourier transform infrared spectrophotometer (model-5300) in Nujol. Raman spectra as reproduced in Fig. 2a of the sample were recorded at the same temperature on a Raman spectrophotometer (Spex-1877) within the region 200–4000 cm^{-1} using the source of excitation as 4880 A^0 line from argon ion (Ar^+) laser. For IR and Raman spectra, the resolution was better than 2 cm^{-1} as well as within the accuracy of ± 2 cm^{-1}.

(B) *Theoretical:* The optimization was carried out of 5-fluoro-uracil using DFT/B3LYP method using the basis set B3LYP/6-311++G** in Gaussian-09 [24], and optimized geometry at B3LYP/6-311++G** level was used for DFT calculation by minimizing the energies of all parameters. The normal vibrational modes have been assigned using the computed modes and related parameters obtained from the visualization program Gauss View-5.09 software [25] of Gaussian-09 program package [24] and PEDs from the GAR2PED [26]. In the optimization, computation has been made for bond lengths, bond angles, vibrational frequencies with the IR intensities (as in Fig. 1b), Raman scattering activities (as in Fig. 2b) and the depolarization

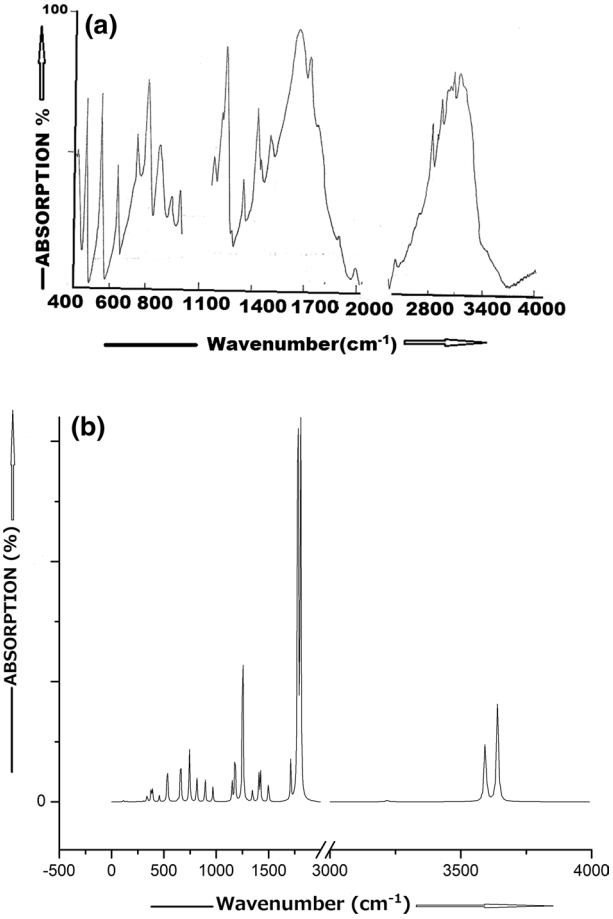

Fig. 1 **a** IR spectrum of 5-fluoro-uracil. **b** Calculated IR spectrum of 5-fluoro-uracil

ratio of Raman bands of 5-fluoro-uracil. The DFT calculations have been used to yield thermodynamics functions and related properties of the biomolecule seen Fig. 3. In visual demonstration, molecular electrostatic potentials (MEPs) predict the reactive sites for the electrophilic/nucleophilic attack to justify the theories of biological activities. HOMO–LUMO analysis for energy gap has been computed using Gaussian-09 [24].

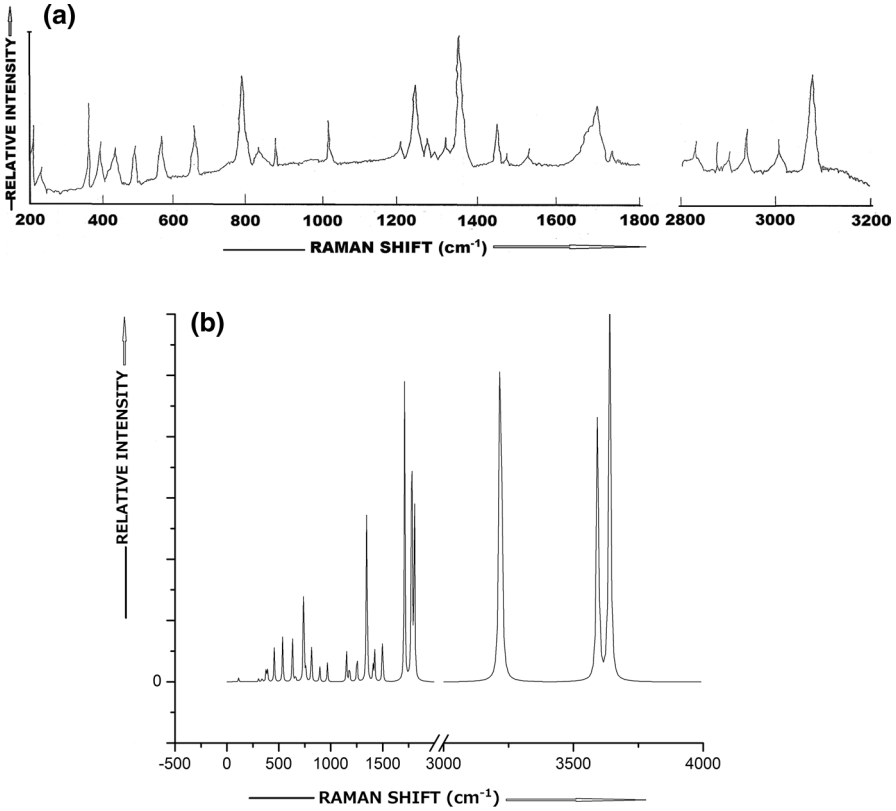

Fig. 2 **a** Raman spectrum of 5-fluoro-uracil. **b** Calculated Raman spectrum of 5-fluoro-uracil

Results and discussion

Molecular charges

The molecular charges are explained as the Mulliken charges which can be obtained on the basis of suitable derived from calculated atomic polar tensor (APT) charges. Cioslowski proposed the other normal definition for the atomic charges which is based on APT invariants [27]. These charges, namely generalized atomic polar tensor (GAPT) charges, have been calculated by Gaussian-09 program package [24] on different basis sets. The calculations are directly related to observed experimental results (i.e., IR intensities). These features contribute to the success of molecular charges as well as understanding the APT and GAPT charges. [28–30].

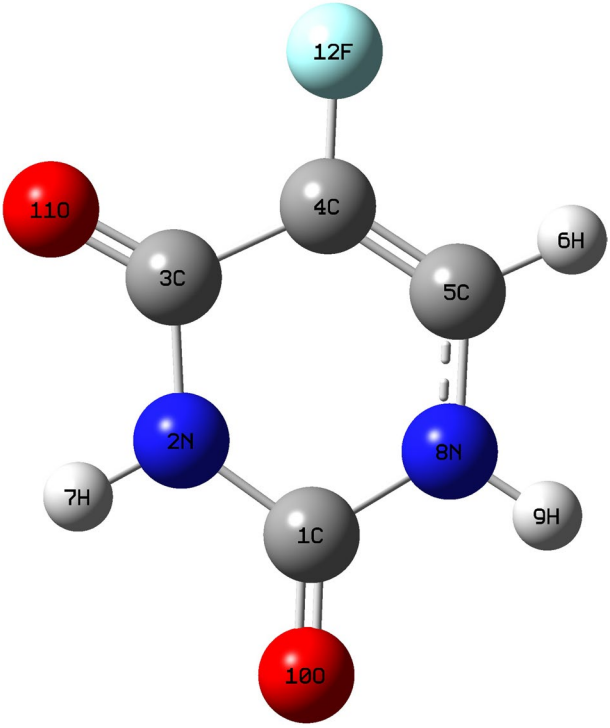

Fig. 3 Numbering of atoms for optimized geometries of 5-fluoro-uracil

APT charges

The atomic polarizability tensor (APT) charges are the sum of charge tensor and sum of charge flux tensor which is known as charge–charge flux model [31]. The atomic charges partially come out on the surface that could be presented the whole chemical properties of the molecule [32, 33]. The optimized geometrical structure and atomic numbering schemes of 5-fluoro-uracil are shown in Fig. 3. The atomic charges on the various atomic site of 5-fluoro-uracil molecule have been computed using the DFT/B3LYP/6-311 ++G** level [24] and are collected in Table 1. The perusal of Table 1 represents the higher electronegativity in comparison with the other atoms. The APT charges of 5-fluoro-uracil have been discussed in comparison with the atomic sites as following. Here, the C_4 atom bears the smallest positive charge with magnitude 0.200664 a.u., and the remaining three carbon atoms of the pyrimidine ring C_1, C_3 and C_5 possess positive charge with magnitudes 1.314133, 1.163170 and 0.371419 a.u., respectively, but only the C_4 atom of pyrimidine ring atoms bears reactant property due to smallest positive charge than other carbon atoms of ring. The two atoms, O_{10} and O_{11}, possess negative APT charges as −0.889341 and −0.821933 a.u. for the molecule. Similar as the two atoms, N_2 and N_8 possess negative APT charges as −0.726606 and −0.688737 a.u. of 5-fluoro-uracil. Due to the high electronegativity, all the O

Table 1 Calculated APT charges[$] and Mulliken atomic charges[$] of 5-fluoro-uracil molecule

S. No.	Atoms[#]	APT charges[$]	Mulliken atomic charges[$]
1	C_1	1.314133	0.329921
2	N_2	−0.726606	−0.389870
3	C_3	1.163170	0.250737
4	C_4	0.200664	−0.228492
5	C_5	0.371419	0.313751
6	H_6	0.093535	0.205528
7	H_7	0.230257	0.363890
8	N_8	−0.688737	−0.363448
9	H_9	0.254480	0.347103
10	O_{10}	−0.889341	−0.338654
11	O_{11}	−0.821933	−0.304451
12	F_{12}	−0.501041	−0.186016

[#]Atomic leveling scheme, as shown in Fig. 3

[$]The taken unit of e

and N atoms have had the negative charges. In the molecule, the 3 H atoms (H_6, H_7, H_9) of 5-fluoro-uracil on pyrimidine possess positive APT charges with magnitudes 0.093535, 0.230257 and 0.254480 a.u., respectively. The F_{12} atom bears negative APT charge as −0.501041 a.u. on the site of atom. Also, it could be noticed that all of the H atoms (H_6, H_7, H_9) on pyrimidine of the molecule are attached directly toward the N atoms and have the positive APT charges.

Mulliken atomic charges

These charges play a crucial role for the DFT calculations in optimized molecular geometry of molecular structure, dipole moment and electronic structure of molecule [31–33]. Mulliken atomic charges of atomic sites as shown in Fig. 3 of 5-fluoro-uracil have been computed using the DFT/B3LYP/6-311++G** basis set [24] and are collected in Table 1 where it could be seen that the three carbon C_1, C_3 and C_5 atoms of pyrimidine ring possess positive charges as 0.329921, 0.250737 and 0.313751 a.u., respectively, except the C_4 atom in Fig. 3 bears negative charges as -0.228492 a.u. due to fluoro group. Both oxygen atoms O_{10} and O_{11} possess negative Mulliken atomic charges as −0.338654 and −0.304451 a.u. for the site of respective atoms. Similar as the two atoms, N_2 and N_8 of 5-fluoro-uracil possess negative Mulliken atomic charges as −0.397268 and −0.360144 a.u. to the respective atoms. Here, all the O and N atoms possess high electronegativity. There are 3 H atoms (H_6, H_7, H_9) of 5-fluoro-uracil on pyrimidine ring possess positive charges as 0.205528, 0.363890 and 0.347103 a.u., respectively. The ring atom F_{12} bears negative Mulliken atomic charge magnitude −0.186016a.u. at site of atom. Here, it is notice that in all of four carbon atoms (C_1, C_3, C_4 and C_5), the C_4 atom has negative charge. But, as discussed above in the case of APT charges, the C_4 atom has positive charge.

Molecular geometry

The atomic labeling scheme and optimized geometrical structure corresponding to the 5-fluoro-uracil biomolecule are shown in Fig. 3. These optimized structural parameters of 5-fluoro-uracil are collected in Table 2. The optimized structures of pyrimidine ring of the 5-fluoro-uracil show that the all ring bonds have been found as the partial double bond character. It could be seen in Table 2 that the optimized bond lengths of ring, the four C-N bond lengths having the descending order (N_2–C_3, N_8–C_1, N_2–C_1 and C_5–N_8), are mostly similar in their magnitudes and lying between bond length ~ 1.41 Å to ~ 1.38 Å. As well as, the rest two C_3–C_4 and $C_4 = C_5$ bond lengths are lying in the ring of plane with order $(C_3–C_4) > (C_4 = C_5)$ in their magnitudes ~ 1.47 Å and ~ 1.34 Å to respective bond. Outer C_4–F_{12} bond has bond length 1.3399 Å. Similarly, it is notice that the internal angles C–N–C, C–C–C and C–C–N of pyrimidine ring are found to be not same, having the smallest $\alpha(N_2–C_3–C_4)$, angle value 112.03^0 and largest $\alpha(C_1–N_2–C_3)$, angle value 128.78^0 to the molecule. The twenty-four dihedral angles are $\sim 0^0 \pm 0.1$ or $\sim 180^0 \pm 1.0$, which represent that the all twelve atoms of 5-fluoro-uracil, C_1, N_2, C_3, C_4, C_5, N_8, O_{10}, O_{11}, H_6, H_7, H_9 and F_{12} are in the same plane as uracil ring. The above results show that all atoms in the ring of pyrimidine for biomolecule lie in a plane.

Vibrational assignments

For the spectroscopic investigation, here, the vibrational spectra of uracil derivatives are taken as the substituent of fluoro group at the *fifth* position of uracil pyrimidine ring. This article is an extensive vibrational spectroscopic study of 5-fluoro-uracil on the *fifth* place of uracil pyrimidine ring where the mass and electronegativity of having order hydrogen < fluorine atom. It deals both the experimental and theoretical vibrational analyses for the 5-fluoro-uracil molecule. Vibrational spectra of biomolecule and their derivatives are very similar to the ring vibration of benzene and their derivatives as well as the pyrimidine ring. This text has been assigned especially for the internal modes in planarity and non-planarity of pyrimidine ring due to the substituent atom or group of atoms that might cause the rising of frequencies which could be due to the mass and electronegativity effect of substituted groups in the place of H atom on the uracil ring. These normal vibrational modes have been analyzed using the computed modes from the visualization program Gauss View-5.09 software [25] of Gaussian-09 program package [24], and PEDs are obtained from the GAR2PED software [26]. The 5-fluoro-uracil molecule has 12 atoms and 30 modes of vibration, which have C_s symmetry, and all of the fundamental modes appear in the IR and Raman spectra. This optimized computation has been made in wavenumbers (cm^{-1}) with the IR intensities (as in Fig. 1b), Raman scattering activities (as in Fig. 2b) and depolarization ratio of the Raman bands which are given in Table 3 for 5-fluoro-uracil molecule. This symmetric study of the computed and observed fundamental vibrational modes of 5-fluoro-uracil molecule is collected along with PEDs in Table 3 as shown Fig. 3 in the following sections:

Table 2 Optimized geometrical parameters of 5-fluoro-uracil

Definition[#]	5-fluoro-uracil
Bond lengths (r) in unit of Å	
r(N_2–C_1)	1.3887
r(N_8–C_1)	1.3895
r(C_1–O_{10})	1.2114
r(N_2–C_3)	1.4075
r(N_2–H_7)	1.013
r(C_3–C_4)	1.4633
r(C_3–O_{11})	1.2105
r(C_4=C_5)	1.3428
r(C_4–F_{12})	1.3399
r(C_5–H_6)	1.0817
r(C_5–N_8)	1.3787
r(N_8–H_9)	1.0088
Bond angles(α) in degree (°)	
α(N_2–C_1–N_8)	112.8916
α(N_2–C_1–O_{10})	123.9377
α(N_8–C_1–O_{10})	123.1707
α(C_1–N_2–C_3)	128.778
α(C_1–N_2–H_7)	115.4345
α(C_3–N_2–H_7)	115.7872
α(N_2–C_3–C_4)	112.0278
α(N_2–C_3–O_{11})	121.8637
α(C_4–C_3–O_{11})	126.1085
α(C_3–C_4–C_5)	121.6975
α(C_3–C_4–F_{12})	117.2238
α(C_5–C_4–F_{12})	121.0786
α(C_4–C_5–H_6)	122.0965
α(C_4–C_5–N_8)	120.7224
α(H_6–C_5–N_8)	117.1811
α(C_1–N_8–C_5)	123.8825
α(C_1–N_8–H_9)	115.4601
α(C_5–N_8–H_9)	120.6574
Dihedral angles(δ) in degree (^{0})	
δ(N_8–C_1–N_2–C_3)	− 0.13
δ(N_8–C_1–N_2–H_7)	− 179.96
δ(O_{10}–C_1–N_2–C_3)	179.90
δ(O_{10}–C_1–N_2–H_7)	0.07
δ(N_2–C_1–N_8–C_5)	0.09
δ(N_2–C_1–N_8–H_9)	179.93
δ(O_{10}–C_1–N_8–C_5)	− 179.94
δ(O_{10}–C_1–N_8–H_9)	− 0.05
δ(C_1–N_2–C_3–C_4)	0.07
δ(C_1–N_2–C_3–O_{11})	− 179.90

Table 2 (continued)

Definition[#]	5-fluoro-uracil
$\delta(H_7–N_2–C_3–C_4)$	179.90
$\delta(H_7–N_2–C_3–O_{11})$	− 0.06
$\delta(N_2–C_3–C_4–C_5)$	− 0.03
$\delta(N_2–C_3–C_4–F_{12})$	179.99
$\delta(O_{11}–C_3–C_4–C_5)$	180.00
$\delta(O_{11}–C_3–C_4–F_{12})$	− 0.0 4
$\delta(C_3–C_4–C_5–H_6)$	− 179.96
$\delta(C_3–C_4–C_5–N_8)$	0.06
$\delta(F_{12}–C_4–C_5–H_6)$	0.00
$\delta(F_{12}–C_4–C_5–N_8)$	− 179.98
$\delta(C_4–C_5–N_8–C_1)$	− 0.01
$\delta(C_4–C_5–N_8–H_9)$	− 179.99
$\delta(H_6–C_5–N_8–C_1)$	179.98
$\delta(H_6–C_5–N_8–H_9)$	0.01

[#]Atomic leveling scheme, as shown in Fig. 3

3.3.1. C–F modes (3 modes), 3.3.2. C–H modes (3 modes), 3.3.3. N–H modes (6 modes), 3.3.4. C=O modes (6 modes) and 3.3.5. pyrimidine ring modes (12 modes).

C–F modes (3 modes)

The stretching (C–F) mode is found to be appeared in higher frequencies than the aromatic amines. From the comparative study of 5-fluoro-uracil, the stretching (C–F) mode has been reported at ~ 1250 cm^{-1} [7, 16]. Here, the ν (C_4–F_{12}) mode is calculated at 1253 cm^{-1} and it is experimentally observed in IR at 1250 cm^{-1} and in Raman at 1250 cm^{-1} with strong intensity, which is highly mixed up with other ring modes. The β (C–F) mode in-plane has been assigned within the region 300–250 cm^{-1} to the reported works [7, 16]. Here, this region has been represented almost near and below from ~ 300 cm^{-1}. This computed β (C_4–F_{12}) mode has been assigned at 304 cm^{-1} and in Raman at 270 cm^{-1} that is quite below due to the mass and electronegativity of fluoro group, and similarly, the γ (C_4–F_{12}) mode for out-of-plane has been computed at 339 cm^{-1} and in Raman at 340 cm^{-1} to have mixed up with hydrogen bonding.

C–H modes (3 modes)

The ν(C–H) modes are indeed a strong characteristic band for the biomolecules [3], and this appears within region 3000–3300 cm^{-1} [19]. In-plane, the C_5–H_6) and β (C_5–H_6) modes have been computed at 3219 and 1346 and these modes have been observed in the IR at 3065 and 1346 cm^{-1} and in the Raman at—and 1350 cm^{-1}, respectively, in which the $\nu(C_5–H_6)$ mode has a strong appearance in PEDs as a characteristic band. The non-planar γ (C_5–H_6) mode is computed at 894 cm^{-1}, and it is observed in the IR at 880 cm^{-1} and in Raman at 886 cm^{-1}. Here, it has been found

Table 3 Fundamental frequencies* of 5-fluoro-uracil

S. no.	Normal distribution of vibrational modes	Exp. observed spectra (cm^{-1})		Theoretically calculated+ frequencies at the DFT/B3LYP/6-311++G**-09 level	PEDs#	Assignments$ for the characterizations of modes	Species	
		Figure 1a	Figure 2a					
		IR	Raman	5-fluoro-uracil	5-fluoro-uracil		In-plane	Out-of-plane
1.	30 vibrational modes as uracil skeleton =(21 a' + 9 a")	3185 (s)	3184 (vs)	3640 (117.3,94.84) 0.20	ν (N_8- H_9) (100)	ν (N_8– H_9)	a'	
2.		3165 (s)	3160 (vs)	3593 (77.03, 68.88) 0.22	ν (N_2- H_7) (89) + α (C_1-C_2-C_3) (6) - α (C_2-C_3-C_4) (4)	ν (N_2–H_7)	a'	
3.		3065 (ms)	–	3219 (02.89, 108.0) 0.29	10 ν (C_5-H_6) (89) + α (C_2-C_3-C_4) (8)	ν (C_5–H_6)	a'	
4.		1790 (vs)	–	1806 (576.1, 31.73) 0.15	α (C_2-C_3-C_4) (46) + ν C_1=O_{10}) (23) - α (C_1-C_2-C_3) (15) - ν(N_2-C_1) (6) + α(C_3-C_4-C_5) (4)	ν (C_1=O_{10})	a'	
5.		1778 (vs)	1774 (vs)	1780 (821.5, 58.22) 0.30	α (C_1-C_2-C_3) (45) - α (C_2-C_3-C_4) (26) - ν(C_3=O_{11})(17) + α(C_3-C_4-C_5) (3)	ν (C_3=O_{11})	a'	
6.		1710 (s)	1702 (vs)	1711 (49.36, 45.31) 0.06	β(C_5-H_6) (47) - ν(C_4=C_5) (29) + α (C_1-C_2-C_3) (16) - α (C_2-C_3-C_4) (3)	ν(C_4=C_5) ring	a'	
7.		1500 (s)	1502 (ms)	1499 (31.37, 08.20) 0.50	β(N_8-H_9)(25) - α (C_1-C_2-C_3) (21) - ν(N_8 –C_5) (16) - β(C_5-H_6) (11) + ν(C_3–C_4) (5) - ν (N_2 –C_3)(5) + ν C_1=O_{10}) (5) + ν(N_8 –C_1) (4)	β(N_8–H_9)	a'	

Table 3 (continued)

S. no.	Normal distribution of vibrational modes	Exp. observed spectra (cm^{-1})		Theoretically calculated[+] frequencies at the DFT/B3LYP/6-311++G**-09 level	PEDs[#]	Assignments[$] for the characterizations of modes	Species	
		Figure 1a	Figure 2a					
		IR	Raman	5-fluoro-uracil	5-fluoro-uracil		In-plane	Out-of-plane
8.		1405 (s)	1405 (s)	1423 (40.71, 04.41) 0.74	$\beta(C_5\text{-}H_6)(32)+\nu(N_2\text{-}C_1)$ (17) + α (C_2-C_3-C_4) (14) - $\beta(N_2\text{-}H_7)(10)$ - $\nu(C_3\text{–}C_4)$ (6) + $\beta(C_5\text{-}H_6)$ (3)	ν (ring)	a’	
9.		1428 (vs)	1430 (ms)	1407 (28.81, 02.20) 0.72	α (C_1-C_2-C_3) (25) - $\beta(N_2\text{-}H_7)$ (22) - $\nu(N_2\text{–}C_3)$(12) - α (C_2-C_3-C_4) (9) - α(C_3-C_4-C_5) (9) - $\beta(C_5\text{-}H_6)$ (7) + β (C_1=O_{10})(5)	$\beta(N_2\text{–}H_7)$	a’	
10.		1346 (s)	1350 (vs)	1346 (18.48, 31.00) 0.36	25 $\beta(C_5\text{-}H_6)$(63) + α (C_2-C_3-C_4)(13) + α (C_1-C_2-C_3) (12) -α(C_3-C_4-C_5) (6)	β ($C_5\text{–}H_6$)	a’	
11.		1250 (vs)	1250 (vs)	1253 (283.0, 04.53) 0.32	α (C_1-C_2-C_3) (59) - α(C_2-C_3-C_4) (21) + $\nu(C_4\text{–}F_{12})$ (7) - $\nu(N_8\text{–}C_5)$ (4)	ν ($C_4\text{–}F_{12}$)	a’	
12.		1180 (s)	1180 (m)	1180 (90.34, 02.76) 0.32	$\beta(C_5\text{-}H_6)$ (53) + α (C_2-C_3-C_4) (20) + $\nu(N_2\text{-}C_1)$ (9) - α(C_3-C_4-C_5) (9) -4 ν ($N_2\text{–}C_3$)(5)	ν (ring)	a’	
13.		1162 (ms)	1050 (s)	1152 (22.26, 03.70) 0.71	α (C_1-C_2-C_3) (36) - α (C_2-C_3-C_4) (22) - ν (N_2 –C_3) (19.) -25 $\beta(C_5\text{-}H_6)$ (7.) + $\nu(N_8\text{–}C_5)$ (6)	ν (ring) Kekule	a’	

Table 3 (continued)

S. no.	Normal distribution of vibrational modes	Exp. observed spectra (cm^{-1})		Theoretically calculated[+] frequencies at the DFT/B3LYP/6-311++G**-09 level	PEDs[#]	Assignments[$] for the characterizations of modes	Species	
		Figure 1a	Figure 2a					
		IR	Raman	5-fluoro-uracil	5-fluoro-uracil		In-plane	Out-of-plane
14.		970 (ms)	–	968 (17.90, 02.31) 0.33	α (C_1-C_2-C_3) (59) + β(C_5-H_6) (25) - ν (N_8 –C_1)(5) - ν(N_2- C_1)(4)	ν (ring)	a’	
15.		886 (s)	880 (ms)	894 (30.91, 02.13) 0.75	γ (C_5-H_6)(49) - δ(C_1-C_2-C_3-C_4) (36) + δ (C_2-C_3-C_4-C_5) (9) - δ (C_3-C_4-C_5-H_6) (6)	γ (C_5-H_6)		a”
16.		815 (vs)	814 (ms)	814 (34.17, 04.88) 0.12	α (C_1-C_2-C_3)(50) - α (C_2-C_3-C_4) (44)	α (ring) Trigonal bending	a’	
17.		760 (ms)	–	760 (01.78, 01.35) 0.75	δ (C_1-C_2-C_3-C_4) (29) - δ (C_3-C_4-C_5-H_6) (28) - γ(C_3=O_{11}) (21) + γ (C_4 –F_{12}) (8) -γ(C_1=O_{10}) (6) + δ (C_2-C_3-C_4-C_5) (5)	γ (C_3=O_{11})		a”
18.		–	–	745 (61.42, 00.09) 0.75	δ (C_3-C_4-C_5-H_6) (37) - δ (C_1-C_2-C_3-C_4) (28) - γ(C_1=O_{10})(18) - γ (N_2- H_7) (6) + γ(C_5-H_6) (5) + γ(C_3=O_{11}) (4)	γ (C_1=O_{10})		a”
19.		740 (sh)	750 (vs)	739 (12.95, 15.61) 0.04	α (C_2-C_3-C_4) (29) + α(C_3-C_4-C_5) (19) + ν(C_3–C_4) (19) + ν(N_2- C_1) (6) + ν(C_4=C_5)(5) + ν (N_2 –C_3)(4) + β(C_5-H_6) (3) + ν(C_4 –F_{12}) (3)	ν(ring) breathing	a’	

Table 3 (continued)

S. no.	Normal distribution of vibrational modes	Exp. observed spectra (cm^{-1})		Theoretically calculated[+] frequencies at the DFT/B3LYP/6-311++G**-09 level	PEDs[#]	Assignments[$] for the characterizations of modes	Species	
		Figure 1a	Figure 2a					
		IR	Raman	5-fluoro-uracil	5-fluoro-uracil		In-plane	Out-of-plane
20.		660 (s)	655 (vs)	660 (79.81, 00.81) 0.75	γ(N_2- H_7) (77) - δ (C_2-C_3-C_4-C_5)(7) + δ (C_3-C_4-C_5-H_6) (7) - γ (C_4 – F_{12}) (5.) - γ (C_1 = O_{10}) (4)	γ (N_2–H_7)		a”
21.		630 (vw)	630 (sh)	631 (02.21, 05.44) 0.58	α (C_1-C_2-C_3) (51) - α (C_2-C_3-C_4) (29) + β (C_1 = O_{10}) (6) - β (C_3 = O_{11})(5) - β(C_4 –F_{12}) (4)	β (C_3=O_{11})	a’	
22.		530 (ssh)	540 (s)	537 (06.75, 05.21) 0.34	13 α (C_2-C_3-C_4) (73) - α (C_1-C_2-C_3) (22)	α (ring)	a’	
23.		540 (vs)	–	532 (54.92, 00.11) 0.75	γ(N_8-H_9)(90) - γ (N_2- H_7) (7)	γ (N_8–H_9)		a”
24.		460 (vs)	470 (s)	456 (07.66, 03.74) 0.57	α (C_1-C_2-C_3)(50) + α(C_3-C_4-C_5)(25) - α (C_2-C_3-C_4) (20)	α (ring)	a’	
25.		420 (s)	420 (s)	390 (18.67, 01.62) 0.62	α (C_1-C_2-C_3) (26) - α(C_3-C_4-C_5) (22) - β(C_1 = O_{10}) (13) - α (C_2-C_3-C_4) (10) - ν (N_2 –C_3)(9) - ν(N_2- C_1) (7) - β(C_3 = O_{11}) (6)	β (C_1=O_{10})	a’	

Table 3 (continued)

S. no.	Normal distribution of vibrational modes	Exp. observed spectra (cm^{-1})		Theoretically calculated[+] frequencies at the DFT/B3LYP/6-311++G**-09 level	PEDs[#]	Assignments[$] for the characterizations of modes	Species	
		Figure 1a	Figure 2a					
		IR	Raman	5-fluoro-uracil	5-fluoro-uracil		In-plane	Out-of-plane
26.		410 (s)	375 (s)	377 (13.92, 01.27) 0.75	δ (C_2-C_3-C_4-C_5)(38) - δ (C_1-C_2-C_3-C_4) (28) + γ (C_4 –F_{12})(22) + γ(N_8-H_9) (5) + γ(C_3=O_{11}) (4)	δ (ring)		a”
27.			340 (s)	339 (10.31, 00.46) 0.75	γ (C_5-H_6)(51) - γ(N_8-H_9) (2) + γ (C_4 –F_{12}) (17) - δ(C_3-C_4-C_5-H_6)(7)	γ (C_4–F_{12})		a”
28.			270 (ms)	304 (00.83,00.34) 0.52	α (C_2-C_3-C_4) (59) - α (C_1-C_2-C_3)(20) - β(C_4 –F_{12})(10) + β (C_3=O_{11}) (5) + β(C_5-H_6) (4)	β (C_4–F_{12})	a’	
29.			–	146 (00.51,00.01) 0.75	δ (C_3-C_4-C_5-H_6)(57) - δ (C_1-C_2-C_3-C_4) (36) - γ(N_2-H_7) (6)	δ (ring)		a”
30.			200 (s)	113 (01.63,00.41) 0.75	δ (C_1-C_2-C_3-C_4)(37) - γ(N_8-H_9) (36) + δ (C_2-C_3-C_4-C_5)(15) - γ (N_2-H_7)(9)	δ (ring)		a”

[#]The number within the bracket after the mode is % PED. The modes contributing with < 3% are omitted. The atomic numbering scheme is shown in Fig. 3

[*]*vw* very weak, *w* weak, *m* medium, *mw* medium weak, *ms* medium–strong, *s* strong, *vs* very strong, *sh* shoulder, *ssh* strong shoulder. [$]$\nu$ stretching, *s* symmetric, *as* antisymmetric, α angle bending, β in-plane bending, γ out-of-plane bending, δ deformation

[+]The first and second numbers within each bracket represent IR intensity (km/mol e) and Raman scattering activity ($Å^4\ u^{-1}$; where, 1 Å = 1×10^{-10} m and 1u = 1 atomic mass unit = 1.6606×10^{-27} kg) while the number above and below each bracket represent the corresponding calculated frequency (or wavenumber $\equiv\bar{\nu}$; in cm^{-1}) and depolarization ratios of the Raman band, respectively

that the ν(C–H) mode is much more sensitive due to the molecule isolated within the Ar matrix than solid phase of molecule [19]. It could be seen that the above result is similar as reported works [9–21].

N–H modes (6 modes)

Similar to C–H stretching modes, the ν (N–H) modes are also the other strong characteristic band for the biomolecules [3] and this mode appears in the region 3200–3600 cm^{-1}, as well as between theoretical and experimental results, and the discrepancies have been arisen in normal modes of N–H bond due to the involvement of some other modes [19]. In-plane, the ν (N_8–H_9) and ν (N_2–H_7) modes are calculated at 3640 and 3593 cm^{-1} and these modes are observed in IR at 3185 and 3165 cm^{-1} and in Raman at 3184 and 3160 cm^{-1}, respectively, with strong appearance in PEDs as characteristic band. The β (N_8–H_9) and β (N_2–H_7) modes in-plane are computed at 1499 and 1407 cm^{-1}, and these two modes are observed in IR 1500 and 1428 cm^{-1} and in Raman at 1502 and 1430 cm^{-1}, respectively. The non-planar γ (N_2–H_7) and γ (N_8–H_9) modes are calculated at 660 and 532 cm^{-1}, and these modes are observed in IR at 660 and 540 cm^{-1} and in Raman at 655 and—cm^{-1}, respectively. Here, it could be seen that the N–H stretching mode is much more sensitive due to the molecule isolated within the Ar matrix than solid phase of molecule [19]. It is found as similar to reported works [9–21].

C=O modes (6 modes)

These vibrational modes of 5-fluoro-uracil have the six C=O modes, namely ν(C_1=O_{10}), ν(C_3=O_{11}), β(C_1=O_{10}), β(C_3=O_{11}), γ(C_1=O_{10}) and γ(C_3=O_{11}). The 1600–1800 cm^{-1} region of the uracil and its derivatives spectra are the congestion of the involving carbonyl stretching motions and the (C=C) stretch mode [12–18]. The ν (C=O) modes are affected by the H-bonding interaction and shifting in frequencies with annoying Fermi resonance [15–18]. In the present case, the ν (C_1=O_{10}) and ν(C_3=O_{11}) modes are computed at 1806 and 1780 cm^{-1}, respectively, and to have mixed up with other ring modes as shown in PEDs, and these have been observed in the IR at 1790 and 1778 cm^{-1} corresponding to Raman at—and 1774 cm^{-1} to the respective modes and as earlier reported [15–18]. The β(C_1=O_{10}) and β(C_3=O_{11}) modes in-plane bending are computed at 390 and 631 cm^{-1} which are observed in the IR at 420 and 630 cm^{-1} and in the Raman at 420 and 630 cm^{-1}, respectively, as supported to the results [12–18]. For the non-planar, the γ(C_1=O_{10}) and γ(C_3=O_{11}) modes are computed at 745 and 760 cm^{-1} and one of the corresponding modes γ(C_3=O_{11}) has been observed in the IR at 760 cm^{-1}, whereas these modes have mixed up with hydrogen bonding and ring modes.

Pyrimidine ring modes (12 modes)

Similar to phenyl ring, the ring of 5-fluoro-uracil has *twelve normal modes* of vibration, namely the *six modes* for ring stretch, *three modes* in-plane for the ring deformation and *three modes* for ring deformation in the out-of-plane. These stretching

modes of ring are the complex combinations of C=C, C–C and C–N stretching bonds of pyrimidine ring [15–18]. However, due to the spectral congestions of the involvement of carbonyl stretching, hydrogen bonding and other ring motions, all the ring stretching modes have arisen within region 1800–700 cm^{-1} and the stretch (C=C) mode has appeared within region 1800–1600 cm^{-1} as refs [15–23]. In this study, the 6 stretching modes have been calculated at 1711 as $\nu(C_4=C_5)$, 1423, 1180, 1152 (as Kekule mode), 968 and 739 cm^{-1}(as ring breathing), and consequently, the 1710, 1405, 1180, 1162, 970 and 740 cm^{-1} were observed in the IR with strong intensities corresponding to Raman peaks at 1702, 1405, 1180, 1050 and 750 cm^{-1} almost with medium–strong intensity to the respective modes. Kekule mode (as ν_{14} mode of benzene ring) of 5-fluoro-uracil [16] has been assigned at ~ 1150 cm^{-1}, whereas in the present case, this is assigned at the same magnitude. Similarly, the ring breathing mode of 5-fluoro-uracil has reported at ~ 739 cm^{-1} that is shifted up by ~ 1 cm^{-1} than the 5-fluoro-uracil at ~ 730 cm^{-1} to Ref. [16], and this is almost same to the result. In-plane, the *three* ring deformation modes have been computed at 814 (as trigonal bending), 537 and 456 cm^{-1} and these modes have been observed in IR at 815, 530 and 460 cm^{-1} corresponding to Raman peaks at 814, 540 and 470 cm^{-1}, respectively. The trigonal bending mode of 5-fluoro-uracil [16] has been assigned at 815 cm^{-1}, which is found to have almost same to this result. Here, the *three modes* for ring deformation in the out-of-plane are computed at 377, 146 and 113 cm^{-1} and these calculated modes of Ref. [16] have been 377, 339 and 146 cm^{-1}, respectively, and here, it could be seen that these ring deformation modes in the out-of-plane are corrected to have possible due to the PEDs in lower region.

HOMO and LUMO analysis and energy gap

The molecular orbital's (MOs) theory plays a crucial role in the quantum chemistry studies for investigating electronic, electrical and optical properties of molecules [34]. 5-Fluoro-uracil has 12 atoms and 66 electrons that occupy 33 molecular orbitals, whereas uracil has 12 atoms and 58 electrons occupying with 29 molecular orbitals, in which each MO contains two electrons having with opposite spins as α (↑ spin) and β (↓spin). HOMO–LUMO analysis of energy gap of 5-fluoro-uracil has been made for the reactivity and stability of molecule. The energy levels of HOMO and LUMO suggest the probability of charge distribution and transfer in biomolecule, and this energy gap between the levels supports to study for the active properties in pharmacology. The HOMO acts as donor of electron, which is confined on the bonds C–C, C–N and C–H, but the LUMO acts as acceptor of electron and is located on the bond C=C in the pyrimidine ring so that the transition from HOMO to LUMO motivates the electronic transition from the ring chain bonds (C–C and C–N) of the molecule to the pyrimidine ring bond (C=C). The difference between HOMO and LUMO energy is energy gap that measures the reactivity and stability, and it is usually the lowest energy excitation in a biomolecule. Therefore, this transition represents to the electronic transition from ground to first excited state and it is explained as electron excitation from HOMO to LUMO. The smaller energy gap can be excited more easily. Therefore, the smaller energy gap is more responsible for

intra-charge transfer interaction taking place within the biomolecule and the reason of bioactivity. The larger energy gap causes the high kinetic stability as well as low chemical reactivity; hence, it is unlike to add electrons to a upper level lying LUMO from lower level lying HOMO so that energy gap should be small for any activated complex and feasible reaction [35, 36]. The energy difference from the HOMO to the LUMO has been calculated to be −5.330415 eV for 5-fluoro-uracil. This energy gap represents the transition from ground state to the lowest excited state of biomolecule. This energy gap specifies the properties of optical polarizability, chemical hardness/softness and kinetic stability/reactivity of a molecule. Pictorial energy levels of HOMO–LUMO with frontier diagram for 5-fluoro-uracil are shown in Fig. 4. The computed HOMO and LUMO energies are collected in Table 4 as −7.32199 eV and −1.991575 eV which represent to the lowest energy for 5-fluoro-uracil. The difference between MOs is −5.330415 eV as energy gap for 5-fluoro-uracil that is less than the uracil (−5.61896 eV). Therefore, the energy gap shows that the charge transfer occurs in the molecule. The gap between MOs of the ground state (E_{HOMO}) to first excited state (E_{LUMO}) has been expressed the bioactivity which is based on the intramolecular charge transfer [37, 38].

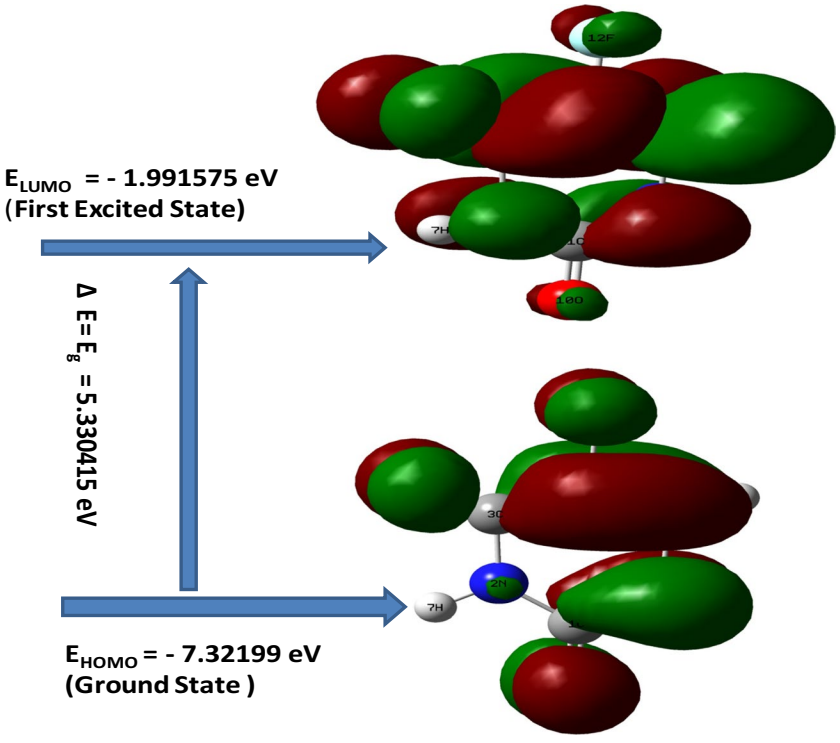

Fig. 4 Pictorial representation of 5-fluoro-uracil with electronic energy levels

Table 4 HOMO–LUMO energy of 5-fluoro-uracil

S. no.	Parameters	Energy (eV)
1.	HOMO (ground state energy)	− 7.32199 eV
2.	LUMO (first excited state)	− 1.991575 eV
3.	HOMO-LUMO(Δ E) = energy gap	− 5.330415 eV

Molecular electrostatic potentials

The molecular electrostatic potentials (MEPs) surface plots of 5-fluoro-uracil are shown in Fig. 5a, which is normally used to study the intermolecular characterization and actions for the drug analysis of molecule. Really, the spatial distributions of Molecular electrostatic potential are responsible to chemical activities in a chemical reaction for an agent at its active sites with strong binding. MEP is related to the atomic charges, dipole moment and chemical reaction activity of biomolecule. In the molecule, MEPs provide a visualized method for understanding the relative polarity through these mappings. The MEPs plots are traced with different colors; red color as most negative electrostatic potential, blue color as most positive electrostatic potential and green color as regions of zero potential in biomolecule. Here, the molecular electrostatic potentials increase in the MEP mapping/arrays in order of colors as red (most −ve), orange (−ve), yellow (less −ve), green (zero) and blue (most +ve). In molecule, the negative electrostatic potential represents for the attraction of proton/cation in red colored region due to high electron density, but positive molecular electrostatic potential represents for the repulsion of proton/cation in blue-colored region due to low electron density (as nuclei regions). In Fig. 5a, the negative regions (as red) indicate as active for nucleophilic reaction, and the electrophilic effect is represented by the positive regions (as blue) of MEPs surface plots. It could be seen from Fig. 5a that the locality of O_{11} atom is placed in orange region and other O_{10} atom is placed in partially red region which reflects the electronegative region and is active site for the nucleophilic reaction. Similarly, the locality of three H atoms on the ring is the region of most positive and is an active site for the electrophilic reaction. The green region represents zero electrostatic potential. In Fig. 5a, it is clearly shown that the near corner of fluoro group shows the partially orange color region as the negative electrostatic potential.

The electrostatic potentials (ESPs) iso-surface plots of 5-fluoro-uracil are shown in Fig. 5b, and the electrostatic potential (ESP) is an important concept to explain the charge distribution as visual variably charged regions in molecule. Here, the charge distribution gives detail information about the action and reaction with other molecules [39, 40]. The electrostatic potential is related to the electron density (ED), and it describes about the sites of electrophilic effect and nucleophilic reaction including the interactions of H bonding [41, 42].

In Fig. 5b, the electrostatic potential (ESP) is an important concept to explain the charge distribution as visual variably charged regions in molecule. Here, the charge distribution gives detail information about the action and reaction with other molecules [39, 40]. The electrostatic potential is related to the electron density(ED), andit

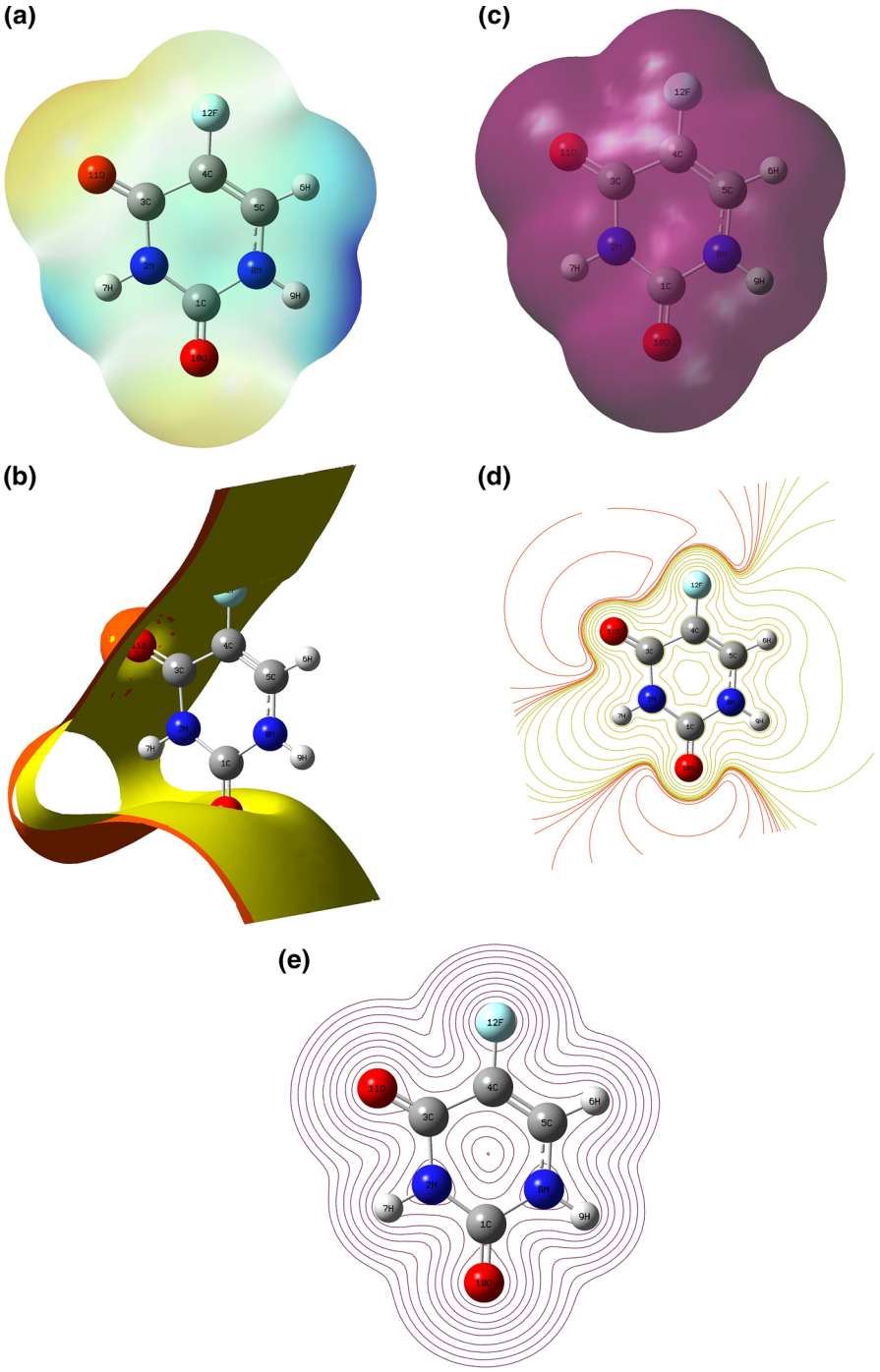

Fig. 5 **a** MEP plot of 5-fluoro-uracil. **b** Iso-surface plot of ESP contour map of 5-fluoro-uracil. **c** Total density mapping of 5-fluoro-uracil. **d** ESP array plot of 5-fluoro-uracil. **e** Total density array plot of 5-fluoro-uracil

describes about the sites of electrophilic effect and nucleophilic reaction including the interactions of H bonding [41, 42]. The red-colored region (as −ve electrostatic potential) represents for the attraction of proton due to high electron density, and the blue-colored region (as +ve electrostatic potential) represents for the repulsion of proton due to low electron density on the ESP surface. The iso-surface for ESP is a surface where the electron density has been specified with a particular value and it represents the electron probability density on specified surface in biomolecule. The electron density iso-surface is shown by coloring with different colors on the iso-surface with contours. Here, the ESP increases with ascending order of colors as red, orange, yellow, green and blue. These iso-surfaces assess the shape, size, charge distribution, reactivity and other properties on site of molecule. At the surface mapping, the regions of electrostatic potentials are represented by red color as the most negative, blue as most positive and green as the zero potential. The graphically electrostatic potential surface is described/defined by Connolly [43–46]. The electron density iso-surfaces with the electrostatic potential surface are shown in Fig. 5b for 5-fluoro-uracil.

Total density mapping, ESP array plot and total density array plot of 5-fluoro-uracil are shown in Fig. 5c, d and e, respectively. These diagrams represent the visual demonstrations for chemical active regions in comparison with reactivity of the atoms in molecule. It could be observed with Fig. 5d that the neighborhood atoms of pyrimidine ring are colored with staging yellow lines as the electronegative which are somewhere more closer and somewhere less closer to each other behavior as nucleophilic/electrophilic properties.

Thermodynamical functions

The translational, rotational and vibrational contribute to thermodynamic functions. In the density functional theory (DFT) calculations, computed wavenumbers have been used to yield thermodynamics functional properties of 5-fluoro-uracil, which are collected in Table 5. The calculated thermodynamical data are

Table 5 Theoretical computed thermodynamic function of 5-fluoro-uracil

S. no.	Parameters	5-fluoro-uracil
1.	Total energy + ZPE(AU)	− 514.122221
2.	Gibb free energy (AU)	− 514.154038
3.	Rotational constants (GHz):	3.19510
		1.40064
		0.97377
4.	Entropy; (calmol^{-1} K^{-1}):	
	Total	83.910
	Translational	40.501
	Rotational	28.691
	Vibrational	14.718
5.	Dipole moments (Debyes)	4.2116

used to correct experimental thermodynamic functions information at 0 K temp and the effect of zero-point vibrational energy. For the zero-point vibrational energy (ZPVE), the scaling factors can be used somewhere to improve their overestimation. The calculated zero-point vibrational energy and free energy are −514.122221 and −514.154038 a.u. for 5-fluoro-uracil. The entropy calculated of the biomolecule is used to correct the experimental thermodynamical data at 0 K temp, and this attributes to avoid of residual or orientation entropy at 0 K temp in the crystal. Here, the translational, rotational and vibrational entropies are 40.501, 28.691 and 14.718 cal mol^{-1} K^{-1} for 5-fluoro-uracil, respectively; hence, the total entropy of biomolecule is 83.910 $calmol^{-1}$ K^{-1}. As well as, the dipole moment of the molecule is 4.2116 Debyes.

All the thermodynamic parameter may be helpful for the further study of related biomolecules. These calculated values in Table 5 are useful for the estimation of directions of chemical reactions and other thermodynamic energies to the biomolecules. Here, it is to be mention that all these thermodynamic calculations were done in gas phase and it could not be used in solution.

Conclusions

All of H atoms on pyrimidine of 5-fluoro-uracil are attached directly with the N atoms and have the positive APT and Mulliken atomic charges. In all of four carbon atoms (C_1, C_3, C_4 and C_5), the C_4 atom has smallest positive APT charge, but C_4 atom has the highest negative Mulliken atomic charge. And the F_{12} atom has had negative APT charges and Mulliken atomic charge. The optimized geometrical structures show that all atoms in pyrimidine ring and on the ring for the molecule lie in a plane.

All the 30 modes have been assigned including the fluoro group modes using the observed IR and Raman spectra and computed related quantities employing the Gaussian-09 and GAR2PED software. In the present case, Kekule mode (as ν_{14} mode) of 5-fluoro-uracil is assigned at ~ 1150 cm^{-1} and similarly the ring breathing at ~ 739 cm^{-1}. Due to the study of PEDs, some of the vibrational modes are corrected to the reported work [16], and the mixing up to the corresponding mode with other modes is shown, respectively.

The computed HOMO–LUMO analysis for energy gap has been carried out, and this study suggests the probability for charge distribution and charge transfer in the biomolecule as well as the pharmacological active property. The molecular electrostatic potentials (MEPs) surface plots and electrostatic potentials (ESPs) iso-surface plots show that the region around the two O atoms is negative potential sites which are the active sites for nucleophilic reaction, and the fluoro group is a negative. Similarly, the locality of three H atoms on the ring is the region of most positive and it is an active place for the electrophilic reaction.

Acknowledgements The corresponding author is grateful to Prof. Saeed Uddin and Dr. Mohd. Shahid Khan, Dept. of physics, JMI, New Delhi (India), for helpful discussion.

References

1. M.D. Kirnos, I.Y. Khudykov, N.I. Alexandrashikina, B.F. Vanyushin, Nature **270**, 369 (1977)
2. F. Michel, M. Hanna, R. Green, D.P. Bartel, J.W. Szostak, Nature **342**, 391 (1989)
3. W.B. Person, Krystyna Szczpaniak, in, ed by J.R. Durig, *Vibrational Spectra and Structure*, vol. 20, Chap. 5 (1993)
4. S. Farquharson, C. Shendre, F.E. Inscore, P. Maksymiuk, A. Gift, J. Raman Spectrosco. **36**, 208 (2005)
5. M.A. Graham, G.W. Lockwood, D. Greenslade, S. Brienza, M. Bayssas, E. Gamelin, Clin. Cancer Res. **6**, 1205 (2000)
6. T. Nakajjma, Word J. Surgery **19**, 570 (1995)
7. B.E. Billinghurst, R. Yeung, G.R. Loppnow, J. Phys. Chem. A **110**, 6185 (2006)
8. H.O. Kim, S.K. Ahn, A.I. Alves, I.W. Beach, J. Med. Chem. **35**, 1987 (1992)
9. V.K. Rastogi, C. Singh, V. Jain, M. Alcolea Palafox, J. Raman Spectrosco. **31**, 1005 (2000)
10. V. Krishnakumar, R. Ramasamy, Spectrochim. Acta **66A**, 503 (2007)
11. Soujanya Yarasi, Brant E. Billinghurst, Glen R. Loppnow, J. Raman Spectrosco. **38**, 1117 (2007)
12. M. Alcolea Palafox, G. Tardajos, A. Guerrero-Martínez, V.K. Rastogi, D. Mishra, S.P. Ojha, W. Kiefer, Chem. Phys. **340**, 17 (2007)
13. V.K. Rastogi, M.A. Palafox, L. Mittal, N. Peica, W. Kiefer, K. Lang, S.P. Ojha, J. Raman Spectrosco. **38**, 1227 (2007)
14. V.K. Rastogi, M. Alcolea Palafox, A. Guerrero-Martínez, G. Tardajos, J.K. Vats, I. Kostova, S. Schlucker, W. Kiefer, J. Mol. Struct. Theochem **940**, 29 (2010)
15. J.S. Singh, J. Mol. Struct. **876**, 127 (2008)
16. J.S. Singh, Spectrochim. Acta A (G.B.) **117**, 502 (2013)
17. J.S. Singh, Spectrochim. Acta A (G.B.) **130**, 313 (2014)
18. J.S. Singh, Spectrochim. Acta A (G.B.) **137**, 625 (2015)
19. L. Lapinski, M.J. Nowak, D.C. Bienkob, D. Michalska, Phys. Chem. Chem. Phys. **4**, 1123 (2002)
20. Barbara Morzyk-Ociepa, Danuta Michalska, Spectrochim. Acta A **59**, 1247 (2003)
21. W.B. Person, K. Szczepaniak, J.S. Kwiatkowski, Int. J. Quantum Chem. **90**, 995 (2002)
22. P.M. El'kin, M.A. Erman, O.V. Pulin, J. Appl. Spectrosc. **73**(4), 485 (2006)
23. M.Y. Choi, R.E. Miller, J. Phys. Chem. **A 111**, 2475 (2007)
24. M.J. Frisch et al., *Gaussian 09, Revision C.01* (G. Inc., Wallingford, 2010)
25. R. Dennington, T. Keith, J. Millam, *GaussView, Version 4.1.2* (Semichem Inc., Shawnee Mission, KS, 2007)
26. J.M.I. Martin, C. Van Alsenoy, *GAR2PED* (University of Antwerp, Belgium, 1995)
27. J. Cioslowski, JACS **111**, 8033 (1989)
28. M. Gussoni, J. Mol. Struct. **141C**, 63 (1986)
29. W.B. Person, J.H. Newton, J. Chem. Phys. **61**(3), 1040 (1974)
30. A. Milano, C. Castiglioni, J. Mol. Struct. Theochem. **955**, 158 (2010)
31. M.M.C. Ferreira, E. Suto, J. Phys. Chem. **96**, 8844 (1992)
32. M.J.S. Dewar, *The Molecular Orbital Theory of Organic Chem* (Mc. Graw- Hill and Inc., New York, 1969)
33. C.A. Coulson, R. McWeeny, *Coulson's Valence* (Oxford University Press, Oxford, 1979)
34. H. Pir, N. Günay, D. Avcı, Y. Atalay, Spectrochim. Acta A **96**, 916 (2012)
35. D.E. Manolopoulos, J.C. May, S.E. Down, Chem. Phys. Lett. **181**, 105 (1991)
36. V. Dixit, R.A. Yadav, Biochem. Pharmacol. (Los Angel) **4**, 183 (2015)
37. L. Padmaja, C. Ravi Kumar, D. Sajan, I.H. Joe, V.S. Jayakumar, G.R. Pettit, J. Raman Spectrosc. **40**, 419 (2009)
38. S. Sagdinc, H. Pir, Spectrochim. Acta, A **73**, 181 (2009)
39. N. Ozdemir, B. Eren, M. Dincer, Y. Bekdemir, Mol. Phys. **108**, 13 (2010)
40. P. Politzer, J.S. Murray, Theor. Chem. Acc. **108**, 13 (2002)
41. F.J. Luque, J.M. Lopez, M. Orozco, Theor. Chem. Acc. **103**, 343 (2000)
42. N. Okulik, A.H. Jubert, Internet electron. J. Mol. Des. **4**, 17 (2005)

43. B. Chattopadhyay, S. Basu, P. Chakraborty, S.K. Choudhuri, A.K. Mukherjee, J. Mol. Struct. **932**, 90 (2009)
44. U.C. Singh, P.A. Kollman, J. Comput. Chem **5**, 129 (1984)
45. M.L. Connolly, Science **221**, 709 (1983)
46. S. Muthu, U. Maheswari, Spectrochim. Acta **92**, 154 (2012)